

SUPPLEMENTARY INFORMATION

Tunable heat generation in nickel-substituted zinc ferrite nanoparticles for effective magnetic hyperthermia

RD Ralandinliu Kahmei* Papori Seal and J.P. Borah

National Institute of Technology Nagaland, India, 797103

* Currently at Indian Institute of Science, Centre for Nanoscience and Engineering, Bangalore, India, 560012

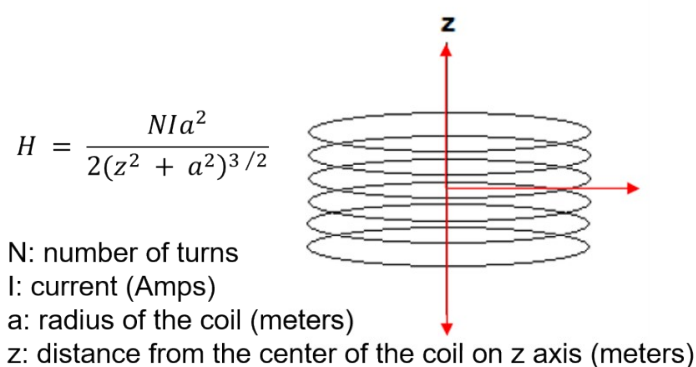


Fig. S1. Schematic for magnetic field calculation

Particle size analysis

Scherrer's equation does not give the accurate crystallite size of the nanoparticles as the FWHM of the XRD peak can be a contribution from both crystallite size and strain; therefore, Williamson-Hall plot was further used here to confirm the crystallite size of the nanoparticles. The W-H plot crystallite size showed values corresponding with that of Scherrer's as shown in Fig. 2 (a) and also in Table S1 below. For a single domain nanoparticle of size < 20 nm, the particle size and crystallite size would be essentially the same. Transmission electron microscopy is useful to get the particle size and to confirm this, TEM of a less magnetic sample (1z) before CTAB coating was done as shown below in Fig. S2. We could only do TEM of sample (1z), as

our TEM lab does not allow magnetic samples. Based on all these analyses, it is convincing that the sizes of the samples are single domain nanoparticles in the range 5-15 nm, considering some agglomeration and non-uniform particle size distribution.

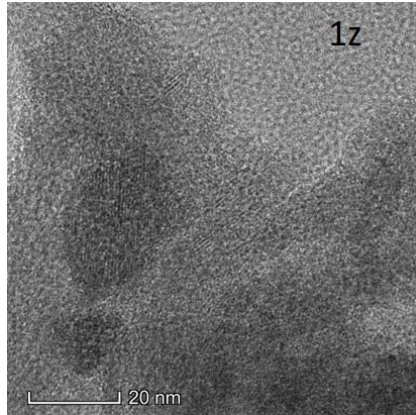


Fig. S2. TEM image of bare $\text{Ni}_x\text{Zn}_{1-x}\text{Fe}_2\text{O}_4$ nanoparticles (1z).

Table S1. Crystallite size from Scherrer's formula and Williamson-Hall equation.

Sample ID	Scherrer (D_{Sch}) (nm)	Williamson-Hall (D_{WH}) (nm)
ZnFe_2O_4	10	7
$\text{Ni}_{0.25}\text{Zn}_{0.75}\text{Fe}_2\text{O}_4$	15	9.8
$\text{Ni}_{0.50}\text{Zn}_{0.50}\text{Fe}_2\text{O}_4$	11	5.7
$\text{Ni}_{0.75}\text{Zn}_{0.25}\text{Fe}_2\text{O}_4$	23	23.7

Lattice parameter analysis

The true value of the lattice parameter was calculated by extrapolating the Nelson Riley function, considering the four most intense peaks ((220), (311), (400), (511), (440)).

The $a \sim f(\theta)$ plot is shown below.

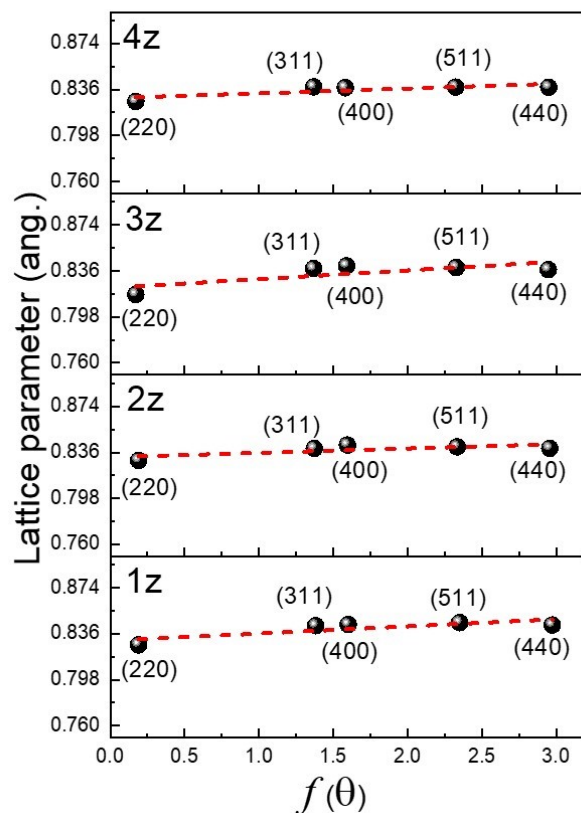


Fig. S3. Nelson Riley plot

FTIR analysis

The intrinsic vibration of the cations and binding of CTAB to the nanoparticles were investigated by FTIR analysis as shown below in Fig. S4. The minor bands around 800 cm^{-1} and 1000 cm^{-1} are assigned to Br^- and out of plane $-\text{CH}$ vibration of CH_3 . A characteristic vibrational symmetric and asymmetric band of N^+-CH_3 is also observed at 1300 and 1600 cm^{-1} in all the four samples. These intense peaks are known to be very sensitive to the inter-chain interactions, which are often used as a key band to check the state of packing of alkyl chain assemblies.¹ Two weak consecutive bands observed in the range of $2000\text{--}2300\text{ cm}^{-1}$ are attributed to the symmetric and asymmetric stretching of the CH_2 group. Superposition of $\nu_s\text{CH}_2$ and $\nu_{as}\text{CH}_2$ can result in deformation of the methylene chain (CH_2 groups) thereby decreasing their intensity.² The broad bands at around $3100\text{--}3400\text{ cm}^{-1}$ in all the samples are due to the stretching mode of H_2O molecules and O-H groups.³ The variations of positions and intensities in the peaks can be ascribed to the alterations of the surface environment in the nanoparticles with the adsorption of

CTAB molecules. These observed bands clearly indicate the interaction of metal surface ions and CTAB molecules. Such interaction engenders lattice strain in the nanoparticles as observed in Fig. 2.

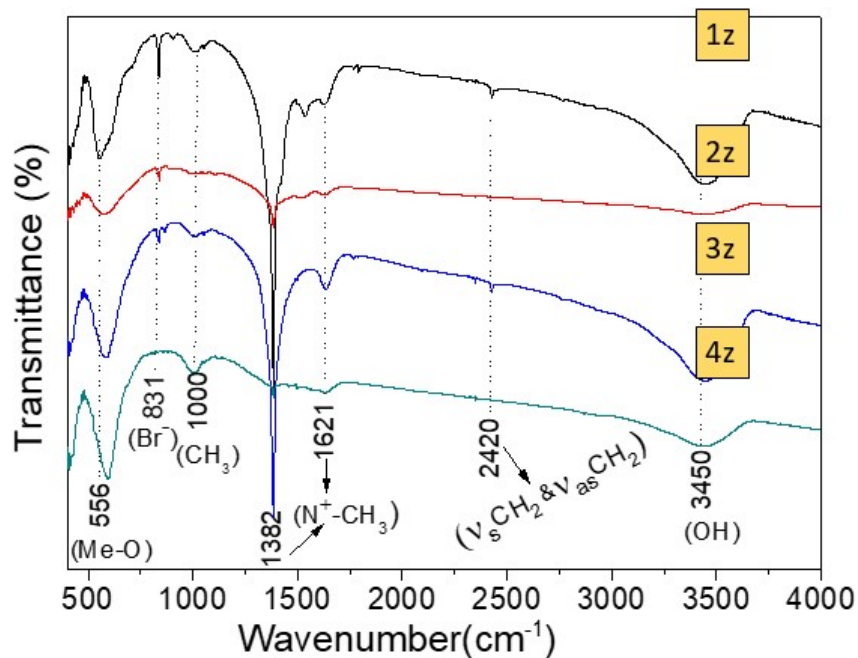


Fig. S4. FTIR absorption bands of CTAB-coated $\text{Ni}_x\text{Zn}_{1-x}\text{Fe}_2\text{O}_4$ nanoparticles.

Raman analysis

Raman spectra is shown in Fig. S5 below with the mode assignment as listed in Table S2.

Table S2. Raman modes of $\text{Ni}_x\text{Zn}_{1-x}\text{Fe}_2\text{O}_4$ nanoparticles

Sample name	$T_{2g}(1)$	E_g	$T_{2g}(2)$	$T_{2g}(3)$	A_{1g}
ZnFe_2O_4	161	249	325	425	643, 710
$\text{Ni}_{0.25}\text{Zn}_{0.75}\text{Fe}_2\text{O}_4$	128	251	318	452	579, 647, 699
$\text{Ni}_{0.50}\text{Zn}_{0.50}\text{Fe}_2\text{O}_4$	158	253	322	470	637, 667, 694
$\text{Ni}_{0.75}\text{Zn}_{0.25}\text{Fe}_2\text{O}_4$	193	276	318	469	639, 666, 690

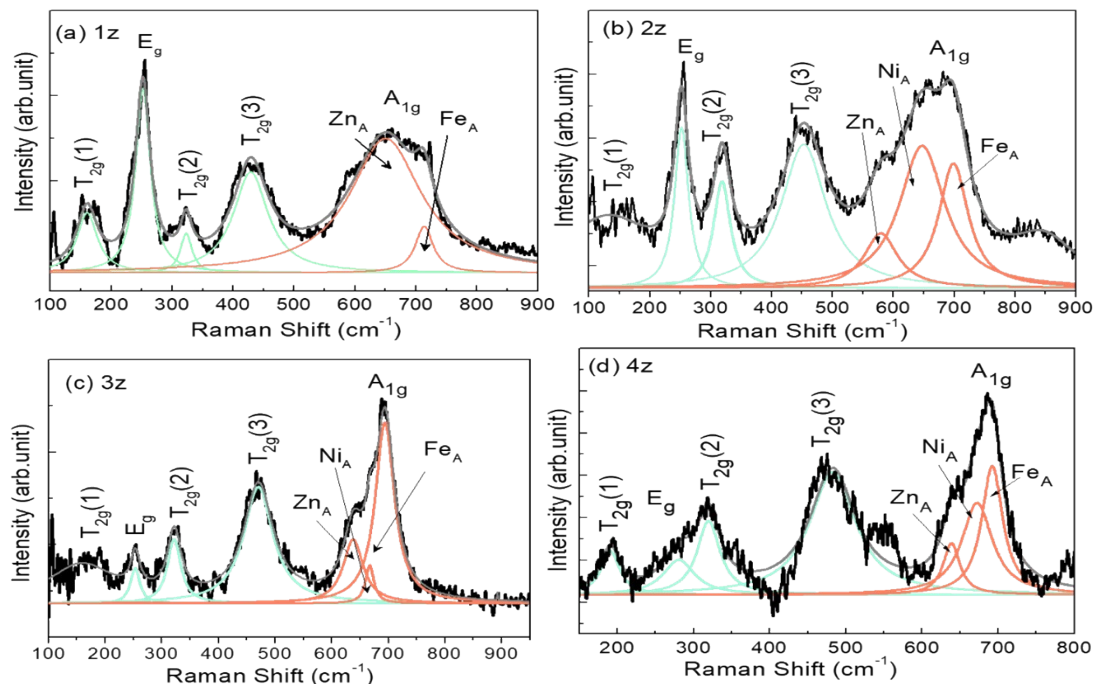


Fig. S5. Raman spectra of CTAB-coated $\text{Ni}_x\text{Zn}_{1-x}\text{Fe}_2\text{O}_4$ nanoparticles.

Magnetic study

A close up range of field dependent magnetization at room temperature (300 K) showing coercivity of < 50 Oe in all the as-prepared samples is shown below in Fig.S6.

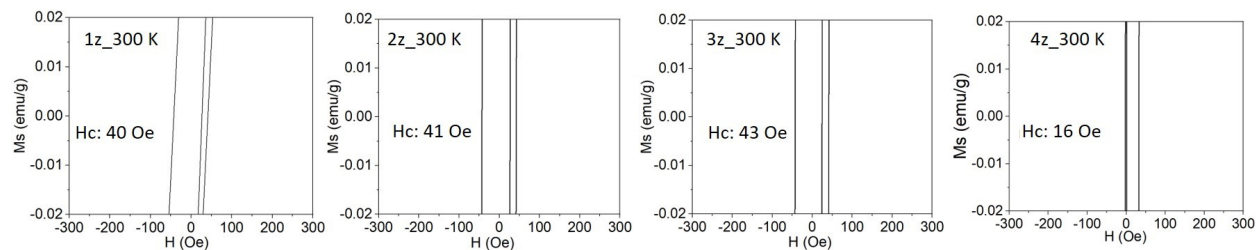


Fig. S6. Coercivity of CTAB-coated $\text{Ni}_x\text{Zn}_{1-x}\text{Fe}_2\text{O}_4$ nanoparticles at 300 K.

References

1. M. Vadivel, R. R. Babu, K. Ramamurthi and M. Arivanandhan, *Ceram. Int.*, 2016, **42**, 19320–19328.
2. K. Khoshnevisan, M. Barkhi, D. Zare, D. Davoodi and M. Tabatabaei, *Synth. React. Inorganic, Met. Nano-Metal Chem.*, 2012, **42**, 644–648.
3. E. C. Mendonça, C. B. R. Jesus, W. S. D. Folly, C. T. Meneses and J. G. S. Duque, *J. Supercond. Nov. Magn.*, 2013, **26**, 2329–2331.